Responses to the referee 1 s' comments

We thank anonymous referee for their comments.

Referee1 s' comments

There are three areas in which I think the authors need to make some important clarifications/ improvements:

1) In Section 3.2, the higher rates of pH decline at depth can be a bit misleading; because pH is on a log scale and pH declines with depth, a given rate of change of pH at depth actually represents a greater rate of change of $[H^+]$ than the same rate would represent at the surface. The authors should consider whether their rates of pH decline at various depths actually represent different rates of $[H^+]$ accumulation.

➔ I agreed. I estimated the rate of the free hydrogen ion concentration ($[H^+]_F$) calculated by using CO2SYS software (Pierrot et al., 2006) at various depths (Suppl. Table 1-1). As the result, the rate of $[H^+]_F$ increase in the in the 26.7–27.0σ_θ layer (1.0×10^{-10} to 2.9×10^{-10} mol kg^{-1} yr^{-1}) was higher than that the acidity rate expected from equilibration with the atmosphere (0.4×10^{-10} mol kg^{-1} yr^{-1}), when it was calculated by using the increase in atmospheric CO_2 (2.1 ppm yr^{-1}) from 1997 to 2011 at 44.4°N (Conway et al., 2012) and constant TA_{win} (2240 μmol kg^{-1}). Similarly, the pH decrease rate in the 26.7–27.0σ_θ layer (–0.003 to –0.005 yr^{-1}) was faster than the acidification rate expected from equilibration with the atmosphere (−0.002 yr^{-1}). Thus, their rates of pH decline at various depths actually represented different rates of $[H^+]_F$ accumulation. Decadal change of maximum pH decline in the subsurface water (-0.05) corresponds to approximately a 10% increase in $[H^+]_F$.

Suppl. Table1-1. Rates of decrease for pH, free hydrogen ion ($[H^+]_F$) and Ω in the western subarctic gyre from 1997 to 2011

Layer	Depth(ave.) [m]	$pH_T^{in\ situ}$	pH_T^{25}	$[H^+]_F$ [mol kg^{-1} yr^{-1}]	$\Omega_{Aragonite}$	$\Omega_{calcite}$
26.7σ_θ	144.0 ± 13.9	-0.0022 ± 0.0010 (p<0.05)	-0.0019 ± 0.0009 (p<0.05)	1.0 ± 0.4 × 10^{-10} (p<0.05)		
26.8σ_θ	172.4 ± 19.1	-0.0036 ± 0.0009 (p<0.0005)	-0.0030 ± 0.0008 (p<0.0005)	1.8 ± 0.4 × 10^{-10} (p<0.0001)	-0.0040 ± 0.0012 (p<0.005)	-0.0064 ± 0.0020 (p<0.005)
26.9σ_θ	215.3 ± 27.9	-0.0051 ± 0.0010 (p<0.0001)	-0.0042 ± 0.0009 (p<0.0001)	2.9 ± 0.6 × 10^{-10} (p<0.0001)	-0.0048 ± 0.0011 (p<0.0001)	-0.0077 ± 0.0018 (p<0.0001)
27.0σ_θ	279.8 ± 33.3	-0.0039 ± 0.0009 (p<.0001)	-0.0032 ± 0.0008 (p<0.0001)	2.5 ± 0.6 × 10^{-10} (p<0.0001)	-0.0035 ± 0.0009 (p<.0005)	-0.0055 ± 0.0015 (p<0.0005)

2) In Section 3.4,the apportioning of DIC changes seems to leave out the potential for divergence of lateral transports (advection) of DIC. Is there evidence for net advective transport of DIC to or from this location?

➔ KNOT and K2 are both located in the western subarctic gyre. The typical water column structure in this region has a minimum temperature layer at about 26.5σ_θ (~100 m), which is the remnant of the mixed layer from the preceding winter; the maximum temperature layer is at about 27.1σ_θ (~370 m) (e.g., Ueno and Yasuda, 2000, Osafune and Yasuda, 2006).

KNOT has occasionally the no minimum temperature water in the water column (~100m) because of the northward migration of subtropical water (Tsurushima et al., 2002). This migrated subtropical water enters the south edge of western subarctic gyre and passes eastward (Ueno and Yasuda, 2000). Because we exclude observed data included no minimum temperature layer as a result of the migration of subtropical water, the combined K2 and KNOT data in this study does not include the subtropical water and is not obviously different in hydrography. Thus, we think that conditions are in place for the stable-state model to be applicable to our analysis.

Moreover, to avoid the effect of advection transportation, we apply salinity-normalized DIC_{win} and TA_{win} values in the minimum temperature layer ($nDIC_{win}$ and nTA_{win}) in calculated method. The rates of oceanic xCO_2 and pH in the winter mixed layer calculated by $nDIC_{win}$ and nTA_{win} are estimated to be 1.3 ± 0.4 ppm yr^{-1} ($p < 0.005$) and −0.0012 ± 0.0004 yr^{-1} ($p<0.001$), respectively, which are consistent with not salinity-normalized results (Fig. 3). nDIC in the winter mixed layer and the 26.9σ_θ surface significantly increased at rate of 1.0 ± 0.2 μmol kg^{-1} yr^{-1} ($p < 0.001$), and 1.8 ± 0.3 μmol kg^{-1} yr^{-1} ($p < 0.001$), respectively. These rates also are consistent with not salinity-normalized results (Fig. 3 and 7). The lack of a ΔS contribution to enhanced acidification in the 26.9σ_θ surface was very low (Table 2 and Figure 6). There is no need to use salinity-normalized values of DIC and TA to correct for such effect, which indicates that there is almost no evidence for net advective transport of DIC to or from this location. Thus, we think that western subarctic gyre remain the stable-state model during the study period.

3) In Section 3.4, changes to DIC driven by remineralization of organic matter (resulting in AOU) are considered. However, fixed stoichiometries of organic matter remineralization are utilized in the calculations. If there have been changes in community structure/foodweb structure over the period of observation, these ratios may not have remained constant. Some quantitative effort to consider the potential effects of changing "Redfield" ratios on the DIC apportionment should be implemented.

➔ We need to consider the potential effects of changing "Redfield" ratios on the DIC change. At first, we examine Redfield ratios f phosphorus and nitrogen to oxygen during the decomposition of organic matter ((P/−O_2), (N/−O_2)) in the 26.9 σ_θ surface, since phosphate, nitrate, AOU increased significantly over the period of observation (0.011 ± 0.002 μmol kg^{-1} yr^{-1}, $p < 0.0001$, and 0.24 ± 0.04 μmol kg^{-1} yr^{-1}, $p< 0.0001$, 1.8 ± 0.4 μmol kg^{-1} yr^{-1}, $p < 0.0001$ respectively). (P/−O_2) and (N/−O_2) are calculated to be 171 ± 38 and 23 ± 4, which nearly are consistent with previous values (170 ± 10, 16 ± 1, Anderson and Sarmiento, 1994). This result indicates that these ratios have remained constant. Thus, the increases of nutrients and AOU on 26.9 σ_θ will be cause by the increase of residence time in the intermediate water. Subsequently, we calculate the carbon to oxygen during the decomposition (C_{org}/-O_2) in the 26.9 σ_θ surface and examine whether bacteria activities in the subsurface change over time or not. In section 3.4, the minimum possible contribution of non–anthropogenic CO_2 (0.8 × 117/170 = 0.55 μmol kg^{-1} yr^{-1}) is the same as the anthropogenic CO_2 uptake (0.5 ± 0.4 μmol kg^{-1} yr^{-1}) in the western subarctic gyre. Considering that minimum estimates of anthropogenic CO_2 and non-anthropogenic CO_2 contributions are of similar magnitude ($\Delta DIC_{air\text{-}sea} = \Delta DIC_{org}$), we estimate ($C_{org}$/-$O_2$) in the 26.9 σ_θ surface from $\Delta DIC_{air\text{-}sea}$ (0.5 μmol kg^{-1} yr^{-1}.) and AOU_{obs} (1.8 μmol kg^{-1} yr^{-1}) according to Eq. (7).

$$\Delta DIC_{org} = (C_{org}/-O_2)\ \Delta AOU_{obs} \quad (7)$$

(C_{org}/-O_2) is calulated to be ~57/170 (0.5/1.8=0.333) and are not consistent with previous values (117/170, Anderson and Sarmiento, 1994). This trial calculation indicates decrease of carbon decomposition efficiency against organic matter, which suggest decline of bacteria activities in the subsurface. However it is not reasonable because observed warming in the 26.9 σ_θ surface (Figure. 6) will enhance bacteria activities in the subsurface. In addition, it almost has been not reported the temporal change of bacteria activities in the subsurface. Thus, it is very difficult whether there have been changes in stoichiometries of organic matter remineralization due to changes in bacteria activities and community structure/foodweb structure over the period of observation or not. This is the subject for a future study which should be solved.

Also I have a few minor issues to point out:

1) Para. 8286 line 3: Revelle Factor should be defined for the non-specialist.

➔ I agreed. I add the definition of Revelle Factor below,

"…high Revelle factor, which is a low CO_2 buffering capacity in seawater, and is characterize…

2) Para. 8288 lines 14-16: There should be parentheses around the stoichiometric ratios for clarity.

➔ I agreed. I add the parentheses around the stoichiometric ratios.

3) Para. 8291, lines 2-3: "...favors the uptake of CO2..."; actually, CO2 is outgassing at this time of year, not being taken up. So instead of "favoring" CO2 uptake you are actually "suppressing" CO2 emission.

➔ I agreed. I rewrite this sentence below.

"… and suppresses the CO_2 emission in the winter mixed layer of western subarctic gyre…"

4) Figures 1,3, 4 and 7 need bigger font sizes to be readable.

➔ I agreed. I make font size in figures 1,3, 4 and 7 bigger, as follows.

5) Figures 2 and 5 need to be resized larger, AND given larger font sizing in order to be readable.

➔ I agreed. I make font size and size in figures 2 and 5 bigger as follows.

Reference

Osafune, S., and Yasuda, I. 2006. Bidecadal variability in the intermediate waters of the northwestern subarctic Pacific and the Okhotsk Sea in relation to 18.6-year period nodal tidal cycle, *J. Geophys. Res*., **111**, C05007, doi:10.1029/2005JC003277.

Ueno, H., and I. Yasuda, 2000, Distribution and formation of the mesothermal structure (temperature inversions) in the North Pacific subarctic region, *J. Geophys. Res*., **105(C7)**, 16,885–16,897.

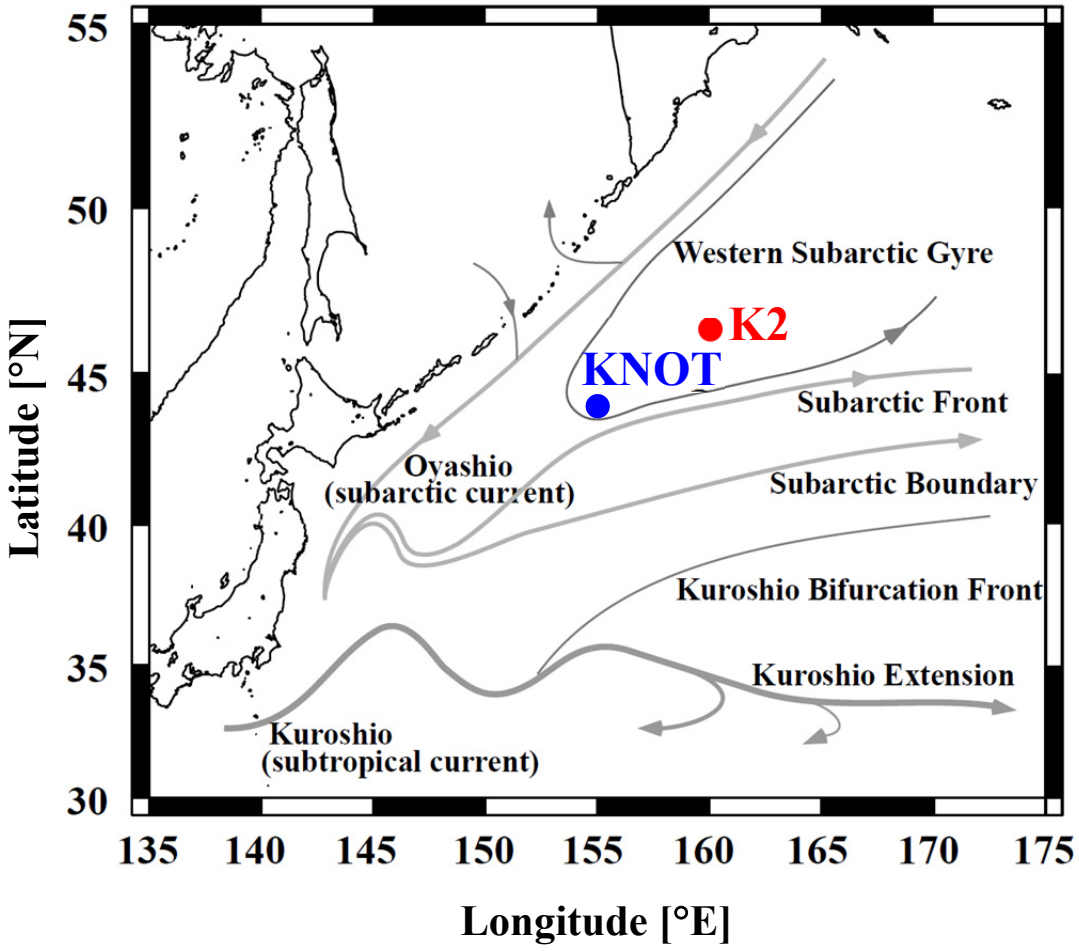

Figure 1. Time-series stations and the main ocean currents in the western North Pacific.

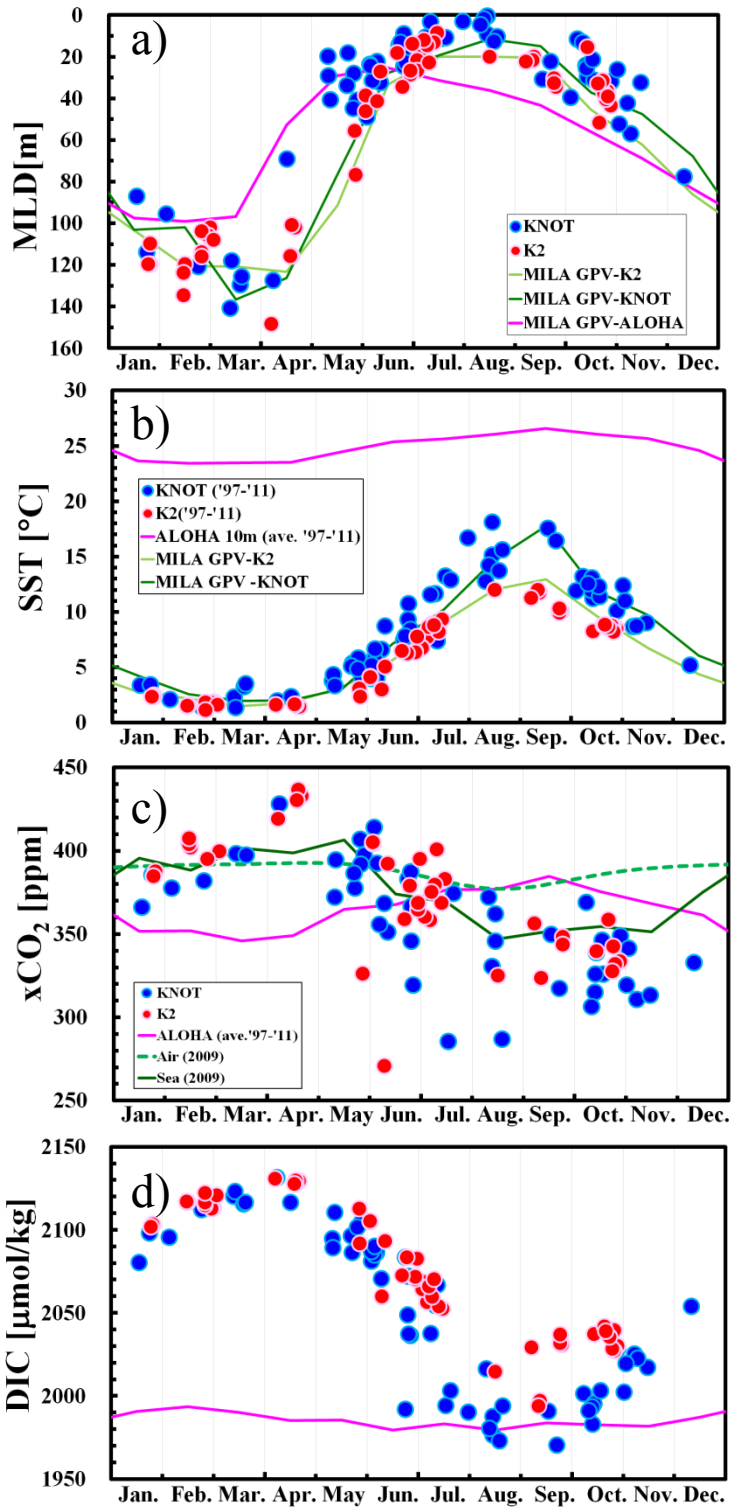

Figure 2. Seasonal variations of (a) the maximum mixed layer depth (MLD), (b) sea surface temperature (SST), (c) oceanic and atmospheric xCO_2, (d) DIC, (e) TA, (f) phosphate, (g) pH (total scale) at the in situ temperature ($pH_T^{in\ situ}$), and (h) $CaCO_3$ saturation states (Ω) with respect to aragonite and calcite in the surface mixed layer at KNOT (blue circles) and K2 (red circles). These figures were plotted using all data from

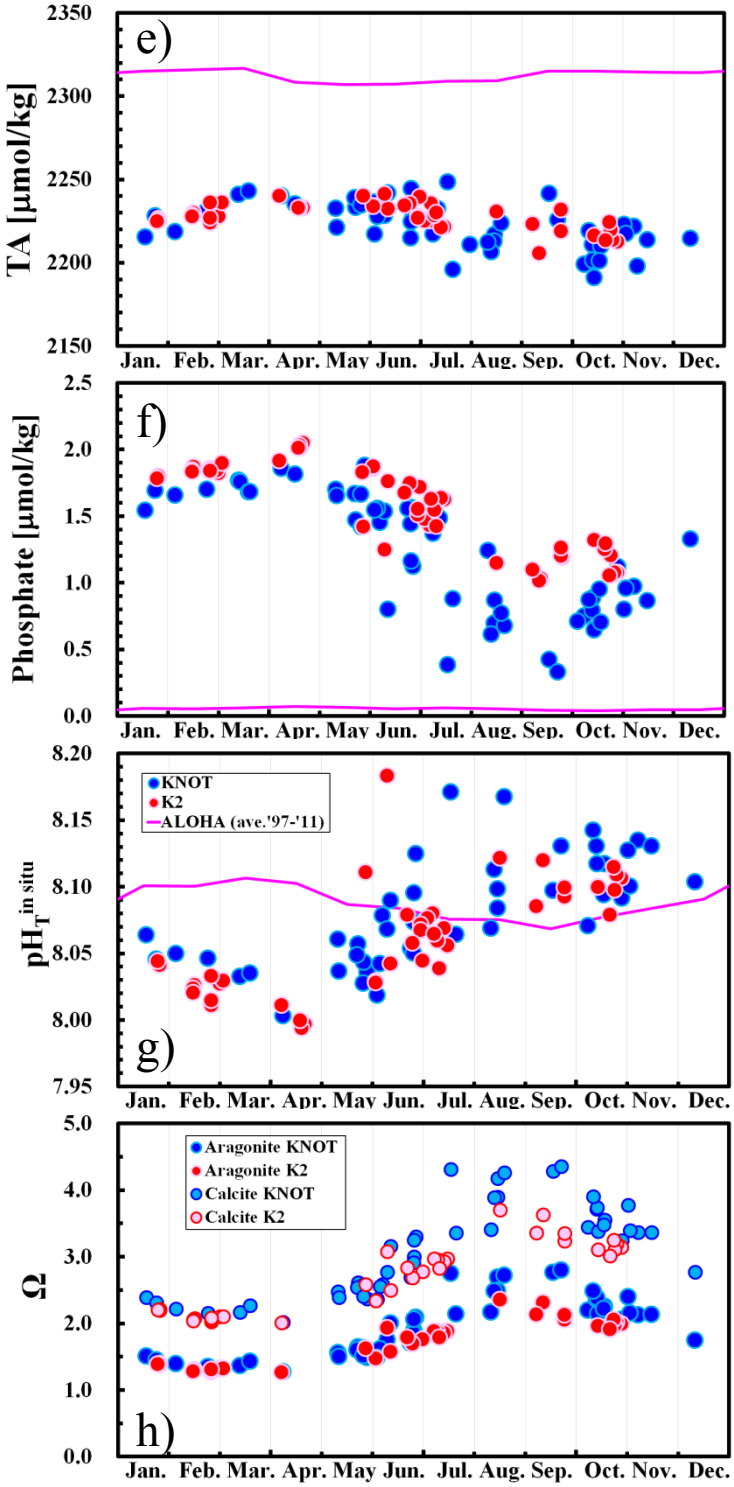

Figure. 2 continued

1997 to 2011 in order to examine typical seasonal variations and for comparison with the climatological monthly means of MIxed Layer data set of Argo, Grid Point Value (MILA GPV) (Hosoda et al., 2010) (a, b), data from Station ALOHA (Dore et al., 2010) (b–g), and Takahashi et al., (2009) (c). Values of oceanic xCO_2 (c), $pH_T^{in\ situ}$ (g) and Ω (h) were calculated from TA and DIC. The density criterion in the surface mixed layer was smaller than 0.125 kg m^{-3} (de Boyer Montégut et al., 2004).

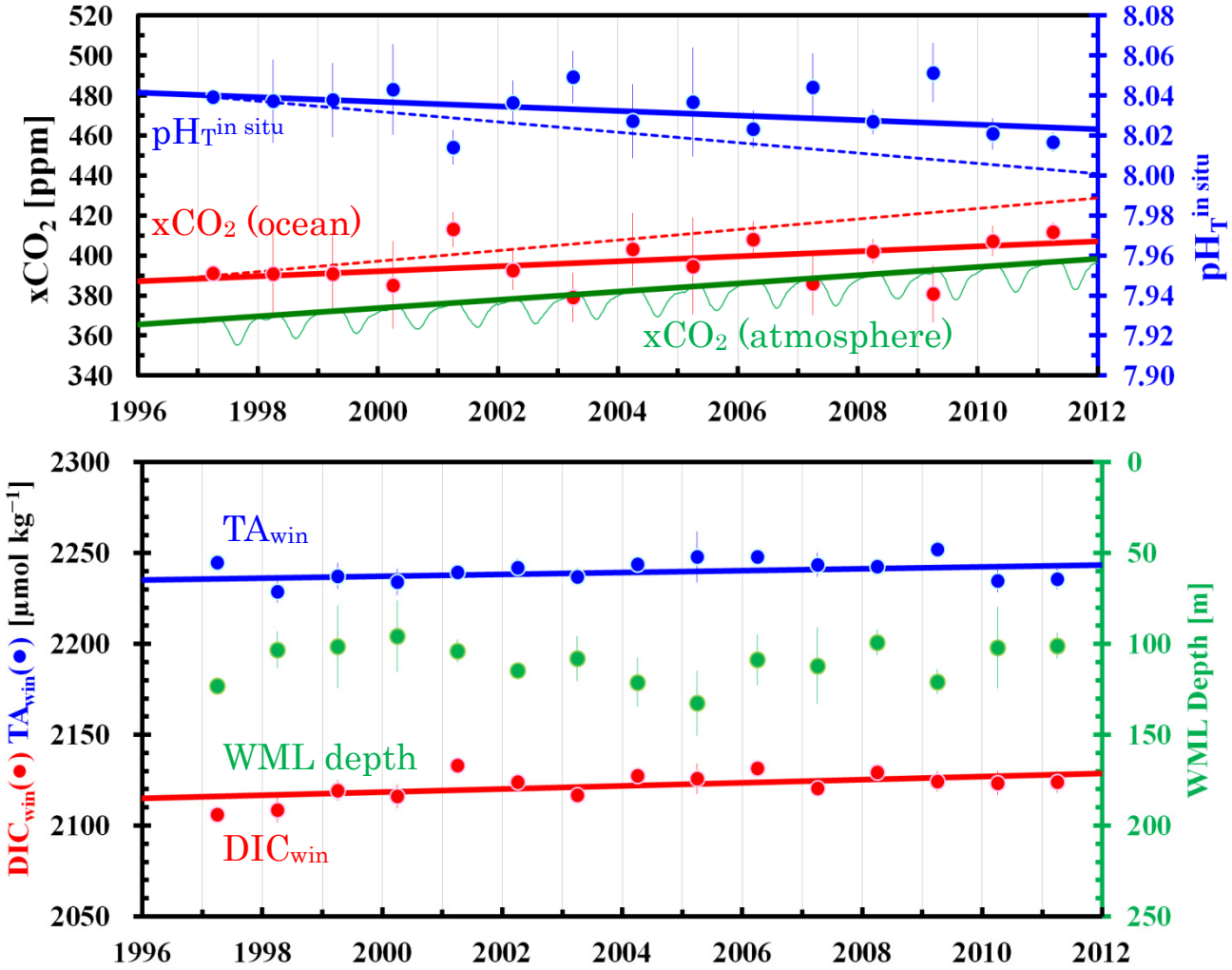

Figure 3. Time-series of $pH_T^{in\ situ}$ (blue circles) and xCO_2 in the ocean (red circles) and the atmosphere (light green curve) at 44.4°N (Conway et al, 2012) (upper panel), and DIC, TA, and depth in the winter mixed layer (DIC_{win}, TA_{win}, WML depth) (lower panel). Regression lines for 1997 to 2011 are shown for $pH_T^{in\ situ}$ (blue line, –0.0011 ± 0.0004 yr^{-1}, $p < 0.01$); oceanic xCO_2 in winter (red line, 1.2 ± 0.4 ppm yr^{-1}, $p < 0.005$); atmospheric xCO_2 in winter (green line, 2.1 ± 0.0 ppm yr^{-1}, $p < 0.001$); TA_{win} (blue line, 0.5 ± 0.2 µmol kg^{-1} yr^{-1}, $p < 0.01$); and DIC_{win} (red line, 0.9 ± 0.2 µmol kg^{-1} yr^{-1}, $p < 0.001$). Regression lines shown for the theoretical $pH_T^{in\ situ}$ (blue dashed line, –0.0026 yr^{-1}) and xCO_2 in the ocean (red dashed line, 2.6 ppm yr^{-1}) were calculated by using increasing values of DIC and constant TA (2240 µmol kg^{-1}).

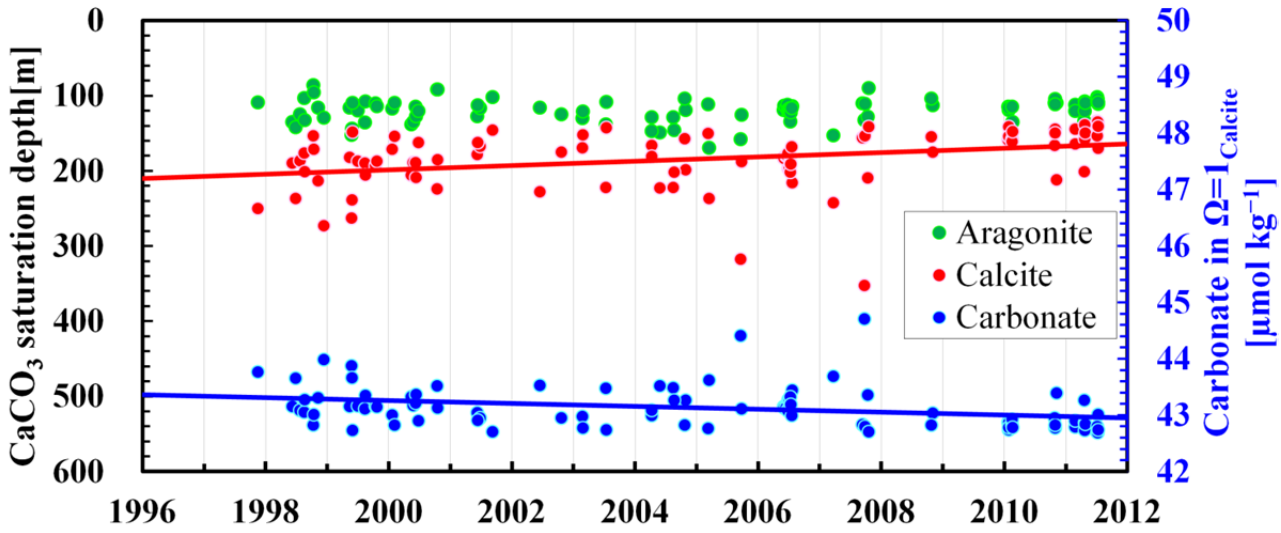

Figure 4. Time-series of the depth of the saturation state of seawater with respect to aragonite (green circles) and calcite ($\Omega_{calcite=1}$; red circles) (left axis), and the concentration of carbonate where $\Omega_{calcite=1}$ (blue circles) in the western subarctic gyre (right axis). Regression lines for 1997 to 2011 are shown for $\Omega_{calcite=1}$ (red line, -2.9 ± 0.9 m yr^{-1}, $p < 0.001$) and carbonate where $\Omega_{calcite=1}$ (blue line, -0.03 ± 0.01 μmol kg^{-1} yr^{-1}, $p < 0.005$).

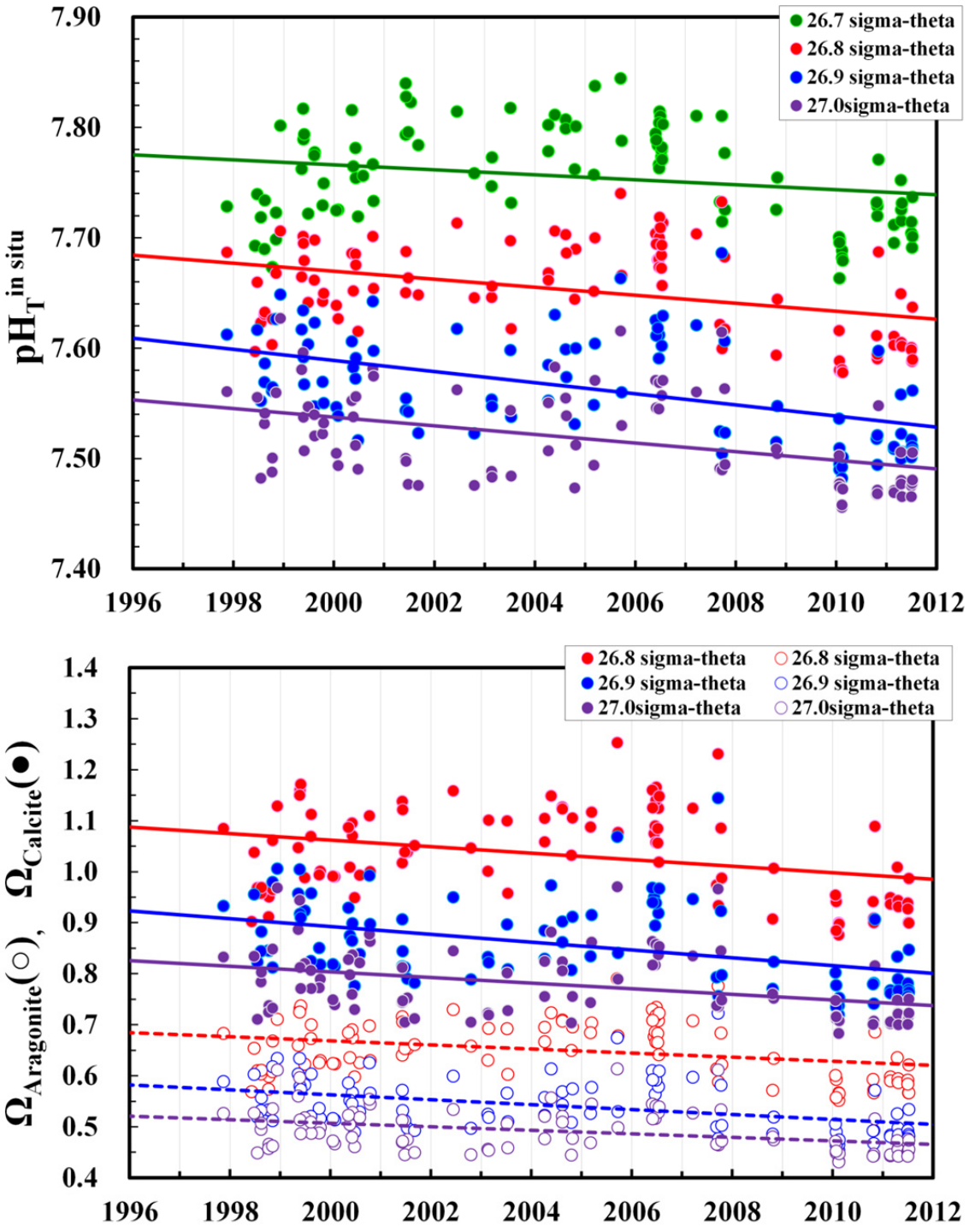

Figure 5. Time-series of $pH_T^{in\ situ}$ (upper panel), and the saturation state of seawater with respect to aragonite ($\Omega_{Aragonite}$, open circles) and calcite ($\Omega_{Calcite}$, closed circles) (lower panel) in the $26.7\sigma_\theta$–$27.0\sigma_\theta$ layer. The regression lines for $pH_T^{in\ situ}$, $\Omega_{Aragonite}$, and $\Omega_{calcite=1}$ decrease significantly from 1997 to 2011. (see Table 1).

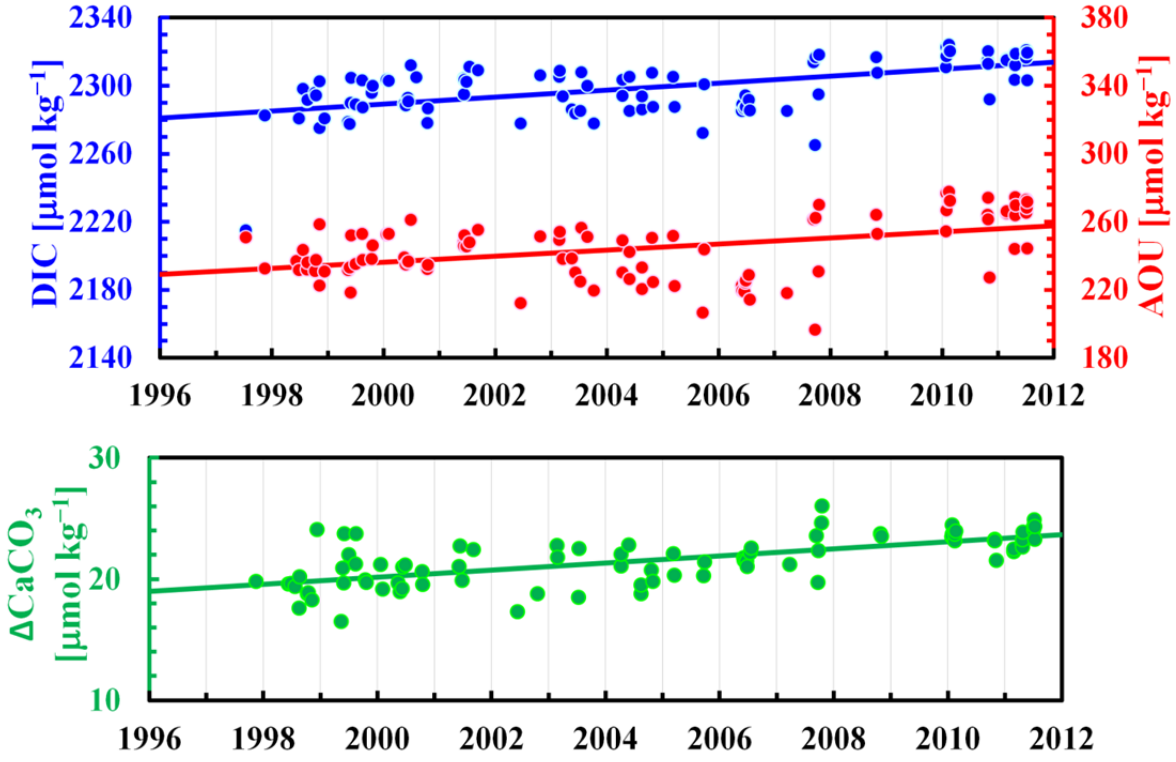

Figure 7. Time-series of DIC (blue circles) and AOU (red circles) (upper panel) and $\Delta CaCO_3$ (green circles) (lower panel) on the 26.9σ_θ surface. Regression lines for 1997 to 2011 are shown for DIC (blue line, 2.0 ± 0.3 μmol kg^{-1} yr^{-1}, $p < 0.001$), AOU (red line, 1.8 ± 0.4 μmol kg^{-1} yr^{-1}, $p < 0.001$) and $\Delta CaCO_3$ (green line, 0.3 ± 0.1 μmol kg^{-1} yr^{-1}, $p < 0.001$).